

Techniques and accuracy of determining the target acceleration from the spectrum of a laser autodyne signal in the presence of nonlinear effects caused by external optical feedback

© M.G. Inkin, D.A. Yakovlev, S.Yu. Dobdin, A.V. Skripal

Saratov National Research State University,
410012 Saratov, Russia
e-mail: sunbeam18.95@mail.ru

Received January 24, 2024

Revised January 24, 2024

Accepted January 24, 2024

Two autodyne (self-mixing) laser interferometry methods for determining microscale-motion parameters are considered, which are based on the analysis of the Fourier spectrum of a laser autodyne signal and use features of the spectra of interference signals from objects moving with a constant acceleration, including a possibility to accurately approximate such spectra by simple functions expressed in terms of the Fresnel integrals. The potential of using these methods under different levels of external optical feedback, which changes the generation conditions of the laser diode, and a relatively high noise level typical of autodyne laser-diode-based interferometers is assessed by means of numerical simulation. The influence of external optical feedback on the spectrum of the signal of an autodyne interferometer from a target moving with a constant acceleration is studied. It is shown that the nature of changes in the spectra of signal fragments with increasing feedback strength makes it possible to use the methods under consideration when the measurements are performed in the weak feedback regime. For both methods, conditions concerning the choice of signal fragments to analyze for achieving good accuracy in estimating motion parameters are found.

Keywords: laser interferometry, laser autodyne, Fourier transform, Fresnel integrals, acceleration measurement, autodyne signal spectrum, optical feedback, self-mixing.

DOI: 10.21883/0000000000

Introduction

The methods of measuring acceleration in micro-displacements based on electrical signals arising from deformation of micro-objects and structures based on them have a low resolution [1,2]. Laser interference and speckle systems have a higher resolution because the laser radiation phase varying with micro-displacements is sensitive to nanometer deformations and displacements. Microelectromechanical acceleration converters with an optical reading unit based on a two-channel Fabry-Perot interferometer [3], Michelson interferometer [4,5], and simultaneously three laser interferometers [6] were created. Some progress in laser acceleration interferometry has been achieved through the use of interferometers with an optical wavelength standard based on Nd:YAG traveling-wave laser with intracavity doubling of the radiation frequency and a stabilization system based on resonances of saturated absorption in molecular iodine [7,8]. A laser interferometer designed to measure the mass velocity of condensed matter in shock wave experiments in the field of high energy density physics can be used for measuring acceleration with an error no worse than $10 \mu\text{m/s}^2$ [9].

Laser autodyne systems have an important advantage over dual-beam interferometers, because they allow creating compact measuring sensors, significantly simplify the

measuring system optical circuit and can be used in MEMS integrated sensors [10–12].

Various methods of analyzing the autodyne signal during the movements of micro-objects with acceleration are known, such as the method of minimizing the discrepancy between the squares of deviations of experimental and theoretical values of the autodyne signal [13,14] and spectral methods for analyzing the shape of the autodyne signal [15].

The possibility of measuring acceleration in case of non-uniformly accelerated micro-displacements of an object, of magnitude from $50 \mu\text{m/s}^2$ and higher, is shown in Ref. [13]. The form of the function of the motion of the reflector with acceleration can also be restored using the methods of the wavelet transform [14].

A method for determining acceleration from the spectrum of an autodyne signal based on the analysis of its discrete Fourier spectrum is proposed in Ref. [16]. This work also showed by numerical modeling that the spectra of the interference signal during the movement of the reflector with acceleration in many cases have a characteristic trapezoidal shape with a well-defined plateau and that the lateral sections of the trapezoidal spectrum can be used to accurately determine the velocity of the reflector at the time moments corresponding to the beginning and end of the analyzed fragment of the signal. The theoretical justification of this method and the criteria for its applicability are presented in this paper. A more general and accu-

rate, although more computationally expensive, alternative method for determining accelerated motion parameters from interference signal spectra is also proposed in this work. Both methods are described in section 2. The main purpose of this work was to evaluate the applicability of these methods in conditions of modulation of the frequency of laser autodyne radiation due to external optical feedback at modulation levels corresponding to very weak and weak feedback modes (sec. 1, 3 and 4).

1. The effect of external feedback on the signal of an autodyne interferometer based on a laser diode

The signal of an autodyne interferometer based on a laser diode is recorded using a photodetector, which is affected by radiation coming from the rear face of the laser diode (Fig. 1, *a*). When the autodyne interferometer operates in the usual interferometric mode, the recorded radiation can be considered as a superposition of the reference wave — wave emitted by the diode from its rear face — and the object wave — the wave that results from the reflection of light emitted by the diode from the front face from an external reflector (the object) and the passage of reflected light through the resonator of the diode, without taking into account any impact of the object wave on the reference wave. In this case, the dependence of the normalized variable (interference) component of the interferometer signal on time *t* in case of movement of external reflector

can be represented as:

$$P(t) = \cos(\omega_0\tau(t)), \tag{1}$$

where ω_0 is the circular frequency of laser radiation, and τ is the time for the object wave to travel the distance from the front face of the diode to the reflector and back. This mode is implemented if the intensity of the object wave is very low when it passes through the diode resonator. In this case, the interference component of the recorded signal is also very small, which often makes this mode unsuitable for measurements. In practice, the modes of very weak and weak external optical feedback are more interesting. In case of increase of the intensity of the subject wave its presence in the diode resonator results in changes of the conditions of generation entailing the modulation of the laser radiation frequency. The effect of change of the frequency of laser diode radiation when radiation reflected from an external reflector enters its resonator is described with good accuracy using the Lang–Kobayashi model [17]. According to this model, the circular frequency of the diode radiation ω under the specified conditions depends on τ and can be found from the equation

$$\omega_0\tau = \omega\tau + C_B \cdot \sin(\omega\tau + \arctg \alpha), \tag{2}$$

where α is the broadening coefficient of the generation line, C_B is a parameter called the level of external optical feedback, and ω_0 is the frequency of diode radiation in the absence of external optical feedback (i.e. at $C_B = 0$). In this case, the time dependence of the normalized variable component of the interferometer signal can be expressed as follows:

$$P(t) = \cos(\omega(\tau(t))\tau(t)) \tag{3}$$

(the change of the frequency of laser diode generation over time τ is considered negligible, which is quite justified under normal conditions). Examples are given in Fig. 1, *b, c* showing the nature and degree of change of the signal $P(t)$ with an increase of the feedback level for the cases of uniform (Fig. 1, *b*) and uniformly accelerated (Fig. 1, *c*) motions of the reflector. The autodyne interferometer operation mode at $C_B \leq 0.1$ is commonly called the very weak feedback mode, and at $0.1 < C_B < 1$ — weak feedback mode [18]. The usual interference mode (1) is realized at $C_B \approx 0$, when the amplitude of the modulation of the radiation frequency becomes negligible.

Two methods for estimating the parameters of the reflector motion are presented in sec.2, based on the analysis of the Fourier spectra of fragments of the autodyne signal corresponding to phases of uniformly accelerated motion of the reflector. These methods use features of the autodyne signal spectra characteristic of the usual interference mode. Further, the possibilities of using these methods in cases of very weak and weak feedback modes are evaluated based on the results of numerical modeling.

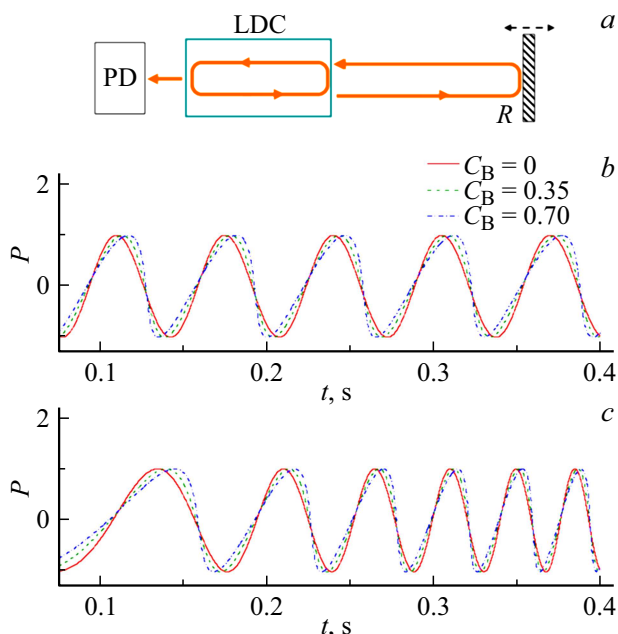


Figure 1. *a* — Schematic of an autodyne interferometer: LDC is the laser diode resonator, *R* is an external reflector (characterized object), PD is a photodetector; *b, c* — changing the waveform of an autodyne interferometer with an increase of the feedback level at uniform (*b*) and uniformly accelerated (*c*) motion of the external reflector. C_B is the external optical feedback level.

2. Spectral methods for estimating reflector motion parameters

Let's briefly focus on the theoretical foundations of the methods for estimating motion parameters considered in this paper.

First, let's clarify the meaning of some terms related to discrete signal spectra, in which they are used in this paper. Let $\{P(t_{sl})\}$ be a sample of values of a signal $P(t)$ corresponding to N values of time within the interval $[t_1, t_2]$:

$$t_{sl} = t_1 + Tl/N, \quad l = 0, 1, 2, \dots, \quad T = t_2 - t_1.$$

We will consider N to be even and large enough that the spectrum calculated for this sample allows for adequate reproduction of the waveform in the interval $[t_1, t_2]$. We will understand the set $\{\mathbf{b}_k\}$ of points $\mathbf{b}_k = (v_k, B_k)$ as the amplitude spectrum of the fragment $[t_1, t_2]$ of the signal for this sample, where v_k are the harmonic frequencies of the discrete Fourier spectrum,

$$v_k = \frac{k}{T}, \quad k = 0, 1, \dots, N/2, \quad (4)$$

and B_k are the amplitudes of the harmonics of the discrete spectrum expressed in terms of the coefficients of the Fourier series representing the values of $P(t)$ of the considered sample

$$P(t_{sl}) = c_0 + \sum_{k=1}^{N/2} \left[c_k \cos\left(2\pi k \frac{l}{N}\right) + s_k \sin\left(2\pi k \frac{l}{N}\right) \right] \quad (5)$$

as follows:

$$B_0 = c_0, \quad B_k = \sqrt{c_k^2 + s_k^2}, \quad k = 1, 2, \dots$$

Coefficients of the series (5) can be calculated with the least computational cost using fast Fourier transform methods. We will also consider the following parameters as amplitude characteristics of the discrete spectrum:

$$V_k = B_k T, \quad k = 1, 2, \dots, N/2 - 1. \quad (6)$$

An ideal normalized autodyne signal in the absence of the feedback effect can be expressed as follows:

$$P(t) = \cos \left[\theta_0 + \frac{4\pi}{\lambda_0} \int_0^t v(t') dt' \right], \quad (7)$$

where $v(t)$ is the instantaneous velocity of the reflector. Let's assume that during the time interval $t_1 \leq t \leq t_2$, the reflector moves with constant acceleration a , and the velocity

$$v(t) = v(t_1) + a \cdot (t - t_1) \quad (8)$$

does not change sign. Substituting (8) in (7), we represent $P(t)$ in the interval $[t_1, t_2]$ as

$$P(t) = \cos \left[\theta_1 + \frac{4\pi}{\lambda_0} \left(v(t_1) \cdot (t - t_1) + \frac{a \cdot (t - t_1)^2}{2} \right) \right], \quad (9)$$

where

$$\theta_1 = \theta_0 + \frac{4\pi}{\lambda_0} \int_0^{t_1} v(t') dt'.$$

Representing the signal as $P(t) = \cos \psi(t)$, we use h to denote the number of cycles in phase increment ψ in the interval $[t_1, t_2]$:

$$h = \frac{\psi(t_2) - \psi(t_1)}{2\pi}. \quad (10)$$

The interval $[t_1, t_2]$ in all examples below was chosen so that h was an integer, and all the numerical estimates given regarding accuracy correspond to this rule for choosing the analyzed signal fragment. Following this rule creates no difficulties in practice: for example, both t_1 and t_2 can be chosen corresponding to the local maxima of the signal ($\cos \theta_1 = 1$), or, say, to zero values of the signal ($\cos \theta_1 = 0$) in the sections with the same sign of the derivative dP/dt .

Exploring the properties of the function

$$\tilde{f}_P(t_1, t_2, v) = \int_{t_1}^{t_2} P(t) \exp(-i2\pi vt) dt$$

with the function $P(t)$ of the form (9), it is possible to find that in cases when both the velocity $v(t_1)$ and the velocity $v(t_2)$ are not very small, or, more precisely, when the below condition is met,

$$\frac{\min\{|v(t_1)|, |v(t_2)|\}}{\lambda_0} > 2.2\sqrt{a_\lambda}, \quad (11)$$

where

$$a_\lambda = \frac{|a|}{\lambda_0},$$

the specific amplitudes of the harmonics of the discrete spectrum V_k (6) can be approximated as follows:

$$V_k \approx KJ(v_k), \quad (12)$$

where

$$K = \frac{1}{2\sqrt{a_\lambda}}, \quad (13)$$

and

$$J(v) = J_F(a_\lambda, v_L, v_U, v) = \sqrt{\left[C\left(\frac{v_U - v}{\sqrt{a_\lambda}}\right) - C\left(\frac{v_L - v}{\sqrt{a_\lambda}}\right) \right]^2 + \left[S\left(\frac{v_U - v}{\sqrt{a_\lambda}}\right) - S\left(\frac{v_L - v}{\sqrt{a_\lambda}}\right) \right]^2}, \quad (14)$$

where

$$C(u) = \int_0^u \cos\left(\frac{\pi}{2}\tau^2\right) d\tau,$$

$$S(u) = \int_0^u \sin\left(\frac{\pi}{2}\tau^2\right) d\tau$$

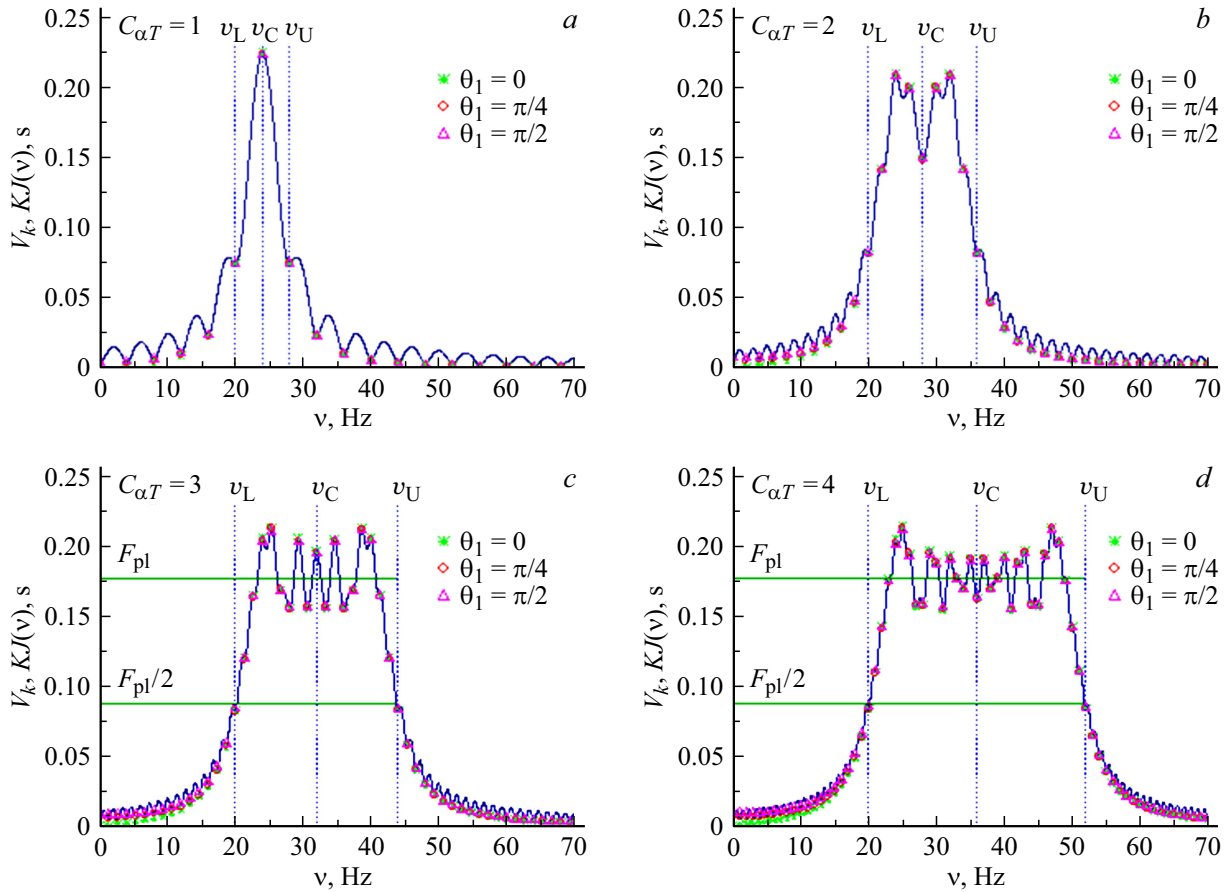


Figure 2. Discrete Fourier spectra of fragments of a signal of the form (9) and the corresponding approximating curves $KJ(\nu)$. The values of the specific amplitudes V_k of discrete spectra calculated at different values of the phase θ_1 are shown by symbols, and the spectra $KJ(\nu)$ are shown by a solid line. Input data are indicated in the text.

are Fresnel integrals, and ν_L and ν_U are characteristic boundary frequencies of the spectrum, defined as

$$\nu_L = \min\{|\nu_1|, |\nu_2|\}, \quad \nu_U = \max\{|\nu_1|, |\nu_2|\},$$

where

$$\nu_1 = \frac{2\nu(t_1)}{\lambda_0}, \quad \nu_2 = \frac{2\nu(t_2)}{\lambda_0}.$$

The frequencies ν_L and ν_U bound the location region of the most significant harmonics of the considered spectrum. This is clearly seen from the examples in Fig. 2. This figure shows the spectra of signal fragments of different durations. The calculation in all cases was performed at $a/\lambda_0 = 16 \text{ s}^{-2}$, $t_1 = 0$, $\nu(t_1)/\lambda_0 = 10 \text{ s}^{-1}$. The values of t_2 were taken as follows: 0.25 (a), 0.5 (b), 0.75 (c) and 1 s (d). In these examples $\nu_L = \nu_1 = 20 \text{ Hz}$. In terms of ν_L , the condition (11) can be reformulated as

$$\nu_L > 4.4\sqrt{a\lambda}. \quad (15)$$

In the considered examples $\nu_L = 5\sqrt{a\lambda}$, i.e. the condition (15) is satisfied. Figure 2 shows the amplitudes V_k calculated for three values of the phase θ_1 , 0, $\pi/4$ and $\pi/2$, and curves $KJ(\nu_k)$. One can see that the approximation

(12) in all the considered cases is good in the main part of the signal spectrum and its high-frequency peripheral part. The accuracy of the approximation (12) slightly deteriorates in the low-frequency peripheral part, with a decrease of frequency ν .

It should be noted that the function $J(\nu)$ is symmetric with respect to $\nu = \nu_C$, where $\nu_C = (\nu_L + \nu_U)/2$, in the sense that for any $\Delta\nu$

$$J(\nu_C + \Delta\nu) = J(\nu_C - \Delta\nu).$$

The following ratio is fulfilled for uniformly accelerated motion

$$\nu_C = \frac{h}{T} \quad (16)$$

(see (10)) and if h is an integer, the harmonic with number h of the discrete spectrum will have a frequency equal to ν_C , as can be seen from (4) and (16). This is one of the advantages of choosing h as an integer. In this case, with good accuracy of (12), the following relations are valid:

$$V_{h+j} \approx V_{h-j} \quad j = 1, 2, \dots \quad (17)$$

(Fig. 2). The symmetry of the discrete spectrum in the sense of fulfilling the ratios (17) can be considered as one of the signatures of the applicability of the approximation (12).

The signal spectra shown in Fig. 2, *c, d* have a characteristic trapezoidal shape with a well-defined plateau. The spectra have this shape when the values of the parameter

$$C_{\alpha T} = \sqrt{a_\lambda T}$$

are about 3 and higher. The value of the parameter $C_{\alpha T}$ determines the shape of the spectrum $J(\nu)$ up to scale (the nature of the change of spectra with an increase of $C_{\alpha T}$ can be estimated from Fig. 2). With $C_{\alpha T} \geq 3$ the values of $J(\nu)$ on plateau fluctuate around the value of $\sqrt{2}$, and the values of $J(\nu_L)$ and $J(\nu_U)$ ($J(\nu_U) = J(\nu_L)$) are approximately two times less than $\sqrt{2}$, the following approximate estimate being valid:

$$\frac{1}{\sqrt{2}} - \frac{1}{2\pi C_{\alpha T}} \leq J(\nu_L), J(\nu_U) \leq \frac{1}{\sqrt{2}} + \frac{1}{2\pi C_{\alpha T}}.$$

The plateau level F_{pl} on the spectra $KJ(\nu)$ shown in Fig. 2, *c, d*, as well as the level $F_{pl}/2$ are shown in these figures by horizontal lines. As can be seen from these figures, the values of $KJ(\nu_L)$ and $KJ(\nu_U)$ in both cases are close to $F_{pl}/2$, which is completely consistent with what was said above regarding the spectra of $J(\nu)$. The said features of trapezoidal spectra $J(\nu)$ with an extended plateau are used in the first of the considered spectral methods for estimating motion parameters, which we will conditionally call MH1.

2.1. MH1 method

The estimates of ν_U or ν_L obtained as follows are used in this method to find the velocities $v(t_1)$ and $v(t_2)$. Let's denote V_k^e values of the amplitudes V_k of the experimental signal spectrum. The values of V_k^e are used in this method as estimates of the values of $KJ(\nu_k)$ (see (12)). The estimate F_{pl}^e of the level of plateau F_{pl} is obtained as the average over amplitudes V_k^e of a certain number of harmonics occurring on the plateau:

$$F_{pl}^e = \frac{1}{n_A} \sum_{k=h-\Delta n_A}^{h+\Delta n_A} V_k^e,$$

where $n_A = 2\Delta n_A + 1$ is the number of harmonics averaged. Next, using linear interpolation over the values of V_k^e an estimate of ν_U (and/or ν_L) is found as the value of ν at which $KJ(\nu) = F_{pl}/2$. For example, the value of ν_{Ue} calculated using the following formula is used as an estimate of ν_U :

$$\nu_{Ue} = \nu_j + \frac{(\nu_{j+1} - \nu_j) \left(\frac{F_{pl}^e}{2} - V_j^e \right)}{V_{j+1}^e - V_j^e},$$

where j and $j+1$ are the numbers of harmonics falling on the high-frequency side of the trapezoidal spectrum and meeting the condition

$$V_j^e > \frac{F_{pl}^e}{2} > V_{j+1}^e.$$

A similar method for estimating the velocities $v(t_1)$ and $v(t_2)$ was previously proposed in Ref. [16] based on the results of numerical experiments. What was said above regarding the signal spectra can be considered as a theoretical justification of the method in Ref. [16] and MH1 can be considered as an improved version of the method [16].

As is clear from the above, the MH1 method is applicable if the condition $C_{\alpha T} \geq 3$ is satisfied for the analyzed signal fragment, which is a serious constraint. The second method, which we conditionally called MG1, is more universal — it is also applicable with significantly lower $C_{\alpha T}$, up to values of the order of one.

2.2. MG1 method

In fact, this method consists in finding such values of the parameters of the function $J_F(a_\lambda, \nu_L, \nu_U, \nu)$ (see (14)), at which the approximation

$$V_k^e \approx KJ_F(a_\lambda, \nu_L, \nu_U, \nu_k)$$

(cf. (12)) is the best for a given frequency range \mathbf{W} . In this case, the parameter K is not considered as a quantity expressed by the formula (13), but simply as a certain proportionality coefficient. The conditions of the problem, namely the fact that the value of $\nu_C = (\nu_L + \nu_U)/2$ and the time T are known, allow it to be solved by considering only one of the parameters as an independent variable, a_λ , ν_L or ν_U , because the other two parameters can be expressed in terms of this parameter and the known parameters ν_C and T . It is convenient to choose ν_U as such an independent variable. The one-parameter family of curves on which the solution of the problem is sought is represented by a function

$$g(\nu_U, \nu) = J_F(a_\lambda(\nu_U), \nu_L(\nu_U), \nu_U, \nu), \quad (18)$$

where ν_L and a_λ are calculated using the formulas

$$\nu_L = 2\nu_C - \nu_U, \quad a_\lambda = \frac{\nu_U - \nu_C}{T}. \quad (19)$$

The frequency range \mathbf{W} can be set (and was set in numerical tests presented below) as a subdomain of some region \mathbf{W}_0 $[\nu_{inf}, \nu_{sup}]$ with specified boundaries so that all harmonics satisfying the following condition fall into the range \mathbf{W} :

$$V_k^e \geq c_{LV} V_{max},$$

where V_{max} is the value of the largest element of the set $\{V_k^e\}$, and c_{LV} is a specified parameter determining the maximum level of harmonics significance (in calculation tests for this work, values of c_{LV} from 0.05 to 0.3 were used), and this condition should be satisfied for the boundary harmonics falling into the region \mathbf{W} . The frequencies of these boundary harmonics, ν_l and ν_m ($\nu_l < \nu_m$) will be considered as the boundaries of the range \mathbf{W} . Mathematically, the search for a solution is reduced to

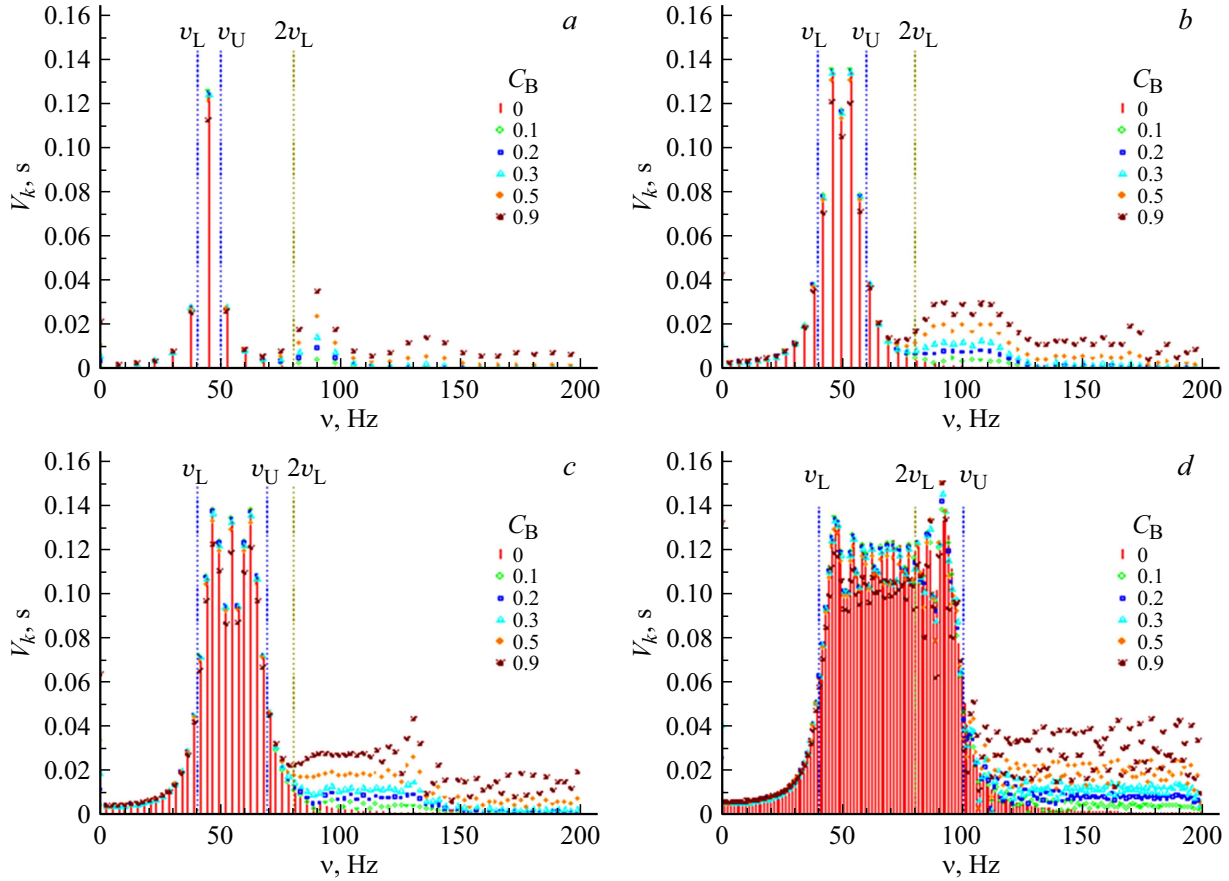


Figure 3. The spectra of the autodyne signal at different durations of the analyzed signal fragment and different values of the feedback coefficient C_B . The amplitudes of the harmonics of the Fourier spectrum with $C_B = 0$ are shown by bars, the amplitudes of the harmonics of the Fourier spectrum for the other values of C_B are shown by symbols. The spectra correspond to the same stage of the reflector motion, but are calculated for time intervals (t_1, t_2) of different duration. The value of t_1 is the same in all cases. The velocity of the reflector at $t = t_1$ is such that $\nu_1 \approx 40$ Hz. The values of t_2 are chosen so that the number of cycles of oscillation of the signal in the interval (t_1, t_2) is an integer, and ν_2 is approximately 50 (a), 60 (b), 70 (c) and 100 Hz (d). Calculations were performed with $a = 25 \mu\text{m/s}^2$ and $\lambda_0 = 0.65 \mu\text{m}$. In this case $\nu_L = \nu_1$, $\nu_U = \nu_2$.

searching for the value of ν_U , at which the global minimum of the function

$$s(\nu_U) = 1 - \frac{\mathbf{g}(\nu_U)^T \mathbf{V}_W^e}{|\mathbf{g}(\nu_U)| |\mathbf{V}_W^e|}, \quad (20)$$

where \mathbf{V}_W^e and $\mathbf{g}(\nu_U)$ are the column-vector of the amplitudes of the harmonics of the experimental spectrum V_k^e and the column-vector of values of $g(\nu_U, \nu)$ respectively,

$$\mathbf{V}_W^e = \begin{pmatrix} V_l^e \\ V_{l+1}^e \\ \vdots \\ V_m^e \end{pmatrix}, \quad \mathbf{g}(\nu_U) = \begin{pmatrix} g(\nu_U, \nu_l) \\ g(\nu_U, \nu_{l+1}) \\ \vdots \\ g(\nu_U, \nu_m) \end{pmatrix}.$$

is reached. The symbol T in (20) denotes transposition; $|\mathbf{V}_W^e|$ and $|\mathbf{g}|$ denote the lengths of the vectors \mathbf{V}_W^e and \mathbf{g} , calculated as

$$|\mathbf{V}_W^e| = \sqrt{\mathbf{V}_W^e T \mathbf{V}_W^e}, \quad |\mathbf{g}| = \sqrt{\mathbf{g}^T \mathbf{g}}.$$

The vectors \mathbf{V}_U^e and $\mathbf{g}(\nu_U)$ are parallel and $s(\nu_U) = 0$ in case of an ideal approximation. The form of experimental spectra allows setting the search area for ν_U relatively narrow, which makes it possible to find a solution very quickly.

3. Evaluation of the accuracy of the methods

One of the tasks of this work was to evaluate the accuracy of determining the reflector movement parameters using the two presented methods at different degrees of manifestation of the feedback effect. The relative error of determining the acceleration, $\delta_{(a)}$, was considered as the main characteristic of the accuracy of the method. It was calculated as

$$\delta_{(a)} = \frac{|a_{\lambda(t)} - a_{\lambda(e)}|}{|a_{\lambda(t)}|} \cdot 100\%,$$

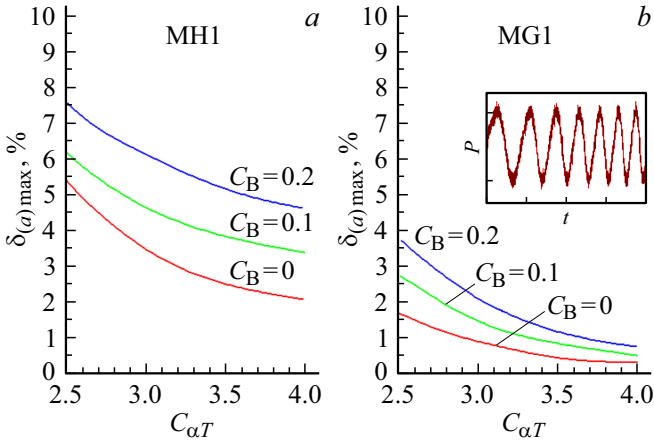


Figure 4. The level of the maximum relative error in determining the acceleration of the reflector by the methods MH1 (a) and MG1 (b) from fragments of a noisy ($P_{\text{Noise}} = 0.1$) autodyne signal at feedback parameter equal to C_B 0, 0.1 and 0.2.

where $a_{\lambda(t)}$ is the true value of the parameter a_{λ} , and $a_{\lambda(e)}$ is the value a_{λ} obtained using the method in question. The values of $a_{\lambda(e)}$ were calculated by (19) using the estimate of v_U found by the considered method. Since the accuracy the dependences of the maximum level $\delta_{(a)}^{\max}$ of error $\delta_{(a)}$ achieved with a given $C_{\alpha T}$ on the value of $C_{\alpha T}$ for cases of noiseless and noisy signal were obtained for each of the methods of the acceleration estimation for both methods depends on the shape of the initial spectrum, and the shape of the spectrum is largely determined by the value of the parameter $C_{\alpha T}$ (Fig. 2). The following representation was used to simulate a noisy signal:

$$P(t_i) = P_p(t_i) + P_{\text{Noise}}\Delta_i,$$

where $P_p(t)$ is a function describing the regular component of the signal, the values of which were calculated using the formula (9), P_{Noise} is a parameter characterizing the noise level, and Δ_i is a Gaussian random variable with zero mean and unit variance.

The plateau level was determined by averaging over five harmonics in case of the use of the MH1 method.

4. Results and discussion

Figure 3 shows the spectra of fragments of different durations of noiseless autodyne signals calculated in accordance with (2) and (3) at different values of the feedback coefficient C_B in the range from 0 to 0.9, corresponding to very weak and weak feedback modes. In all cases, the considered fragments meet condition (15), which is why the spectra corresponding to $C_B = 0$ (harmonic amplitudes for this case are shown by bars) are almost perfectly symmetrical and fully suitable for applying approximation (12). The spectra for $C_B = 0.1$ and $C_B = 0.2$ differ markedly from the spectra for the case of $C_B = 0$ only by a slight increase of harmonic amplitudes in the region of $\nu \geq 2\nu_L$. Moreover,

in the cases shown in Fig. 3, $a-c$, the changes almost do not affect the main part of the signal spectrum, since in these cases the main part of the spectrum lies outside the region $\nu \geq 2\nu_L$. In the case shown in Fig. 3, d , the edge of the main part of the spectrum falls into the region $\nu \geq 2\nu_L$, but both at $C_B = 0.1$ and at $C_B = 0.2$ the spectrum changes at this edge are not very significant. Such a nature of the spectrum changes due to the feedback effect at $C_B \leq 0.2$ allows expecting that the accuracy of estimates of motion parameters using both considered spectral methods will not be much worse than in the case of $C_B = 0$. The results of numerical experiments have confirmed the validity of these expectations. The obtained estimates of the maximum error level for determining acceleration by the methods MH1 (a) and MG1 (b) are shown in Fig. 4 for the spectra of a signal with a noise level $P_{\text{Noise}} = 0.1$ (the appearance of a signal with such a degree of noise is shown in the box Fig. 4, b) at $C_B = 0.1$ and 0.2. These estimates were obtained as a result of processing the spectra of more than 6800 fragments of signals in the case of the MG1 method and more than 4700 fragments in the case of the MH1 method at acceleration values of 25 and $50 \mu\text{m/s}^2$ ($\lambda_0 = 0.65 \mu\text{m}$) and initial velocities $v(t_1)$ in the range from 5.6 to $40 \mu\text{m/s}$. Fig. 4 shows that the error of determination of acceleration for both methods decreases with the increase of $C_{\alpha T}$. At the same time, the accuracy of MG1 turned out to be significantly higher than the accuracy of MH1 for any given $C_{\alpha T}$ in the field of applicability of the MH1 ($C_{\alpha T} > 2.5$) method. The following values of fitting parameters were used in the specified range in case of the MG1 method: $v_{\text{inf}} = 0$, $v_{\text{sup}} = 200 \text{ Hz}$, $c_{LV} = 0.2$. Unlike MH1, the MG1 method is applicable for analyzing signal fragments for which the value of $C_{\alpha T}$ falls in the range from 1 to 2.3. However, the value c_{LV} should be reduced, for achieving good accuracy when considering the range $1 < C_{\alpha T} < 1.8$. We used $c_{LV} = 0.1$ for this sub-range, which provided the level of accuracy shown in Fig. 4, b . Calculations showed that there are no values c_{LV} at which high accuracy of estimates would be achieved in the entire considered area $1 < C_{\alpha T} < 4$, i.e., a change of c_{LV} in case of the transition from one sub-range to another is inevitable. It should be noted that at speeds $v(t_1)$ close to the specified lower limit and the chosen acceleration values, condition (11) is strongly violated, but even at such initial speeds, the obtained acceleration estimates turned out to be quite adequate. Thus, the numerical experiment showed the applicability of the MH1 and MG1 methods with small values of C ($C_B \leq 0.2$), and even under more general conditions than those determined by the ratio (11).

Calculations showed that the nature of the change of the spectra of signal fragments with an increase of C_B allows the MG1 method to be successfully used even with $0.2 < C_B \leq 0.9$. As already noted, the main changes of the spectra with an increase of the feedback level occur in the region of $\nu \geq 2\nu_L$. This can be explained based on the fact that with a harmonic input (corresponding to $C_B = 0$) signal (see Fig. 1, b for uniform movement

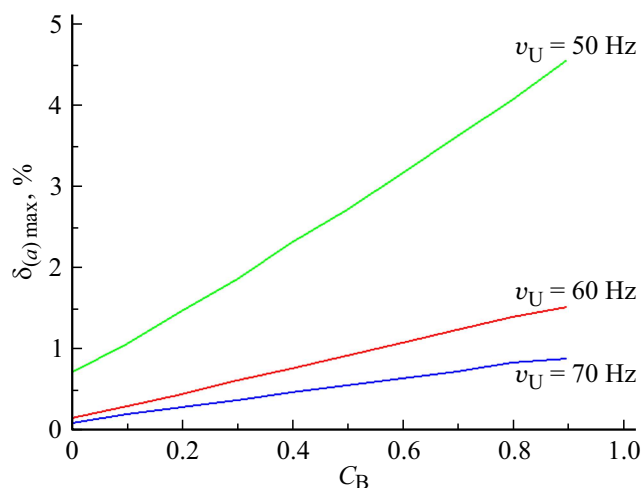


Figure 5. Estimates of the relative error of determination of the acceleration of the reflector by the MG1 method with $\nu_{\text{sup}} = \nu_{\text{BL}}$.

of the reflector) an increase of C_B practically does not interrupt the periodicity of the signal, i.e. it enhances significantly only those harmonics whose frequency is a multiple of the frequency of the original signal. In case of an accelerated motion, as shown by Fig. 3, with an increase of C_B , the region of location of signal harmonics associated with the feedback effect also begins to cover a small transition region adjacent to the region $\nu \geq 2\nu_L$. Let's denote the lower limit of this range ν_{BL} . In the examples in Fig. 3 ν_{BL} is approximately 75 Hz, whereas $2\nu_L = 80$ Hz. In the region $\nu < \nu_{\text{BL}}$, the shape of the spectrum with increasing C_B remains approximately the same as at $C_B = 0$. This allows using the MG1 method with $\nu_{\text{sup}} = \nu_{\text{BL}}$ to estimate acceleration in situations where $\nu_U < 2\nu_L$ (as in Fig. 3, *a–c*), i.e. setting the fitting area **W** outside the region $\nu > \nu_{\text{BL}}$. Curves of dependence of the error in determining acceleration $\delta_{(a)}$ using this technique on C_B for the intervals of movement of the reflector for which the spectra shown in Fig. 3, *a* ($\nu_U = 50$ Hz), *b* ($\nu_U = 60$ Hz), and *c* ($\nu_U = 70$ Hz) were calculated are shown in Fig. 5. The data shown in this figure are obtained for noiseless signals. In calculations with noise level of $P_{\text{Noise}} = 0.1$, the error δ_a increased by approximately 0.5% in the cases of $\nu_U = 60$ and 70 Hz and by 0.5–1% in the case of $\nu_U = 50$ Hz.

Conclusion

Therefore, the analysis and the presented data show that both considered spectral methods for determining the parameters of the reflector motion from the laser autodyne signal can be successfully used in conditions of significant modulation of the radiation frequency due to the passage of the object wave through the resonator of the laser diode, the MH1 method at feedback levels $C_B \leq 0.2$, the MG1 method at feedback levels $C_B \leq 0.9$. In case of usage of the second method in modes with $C_B > 0.2$, analyzed

signal fragments should be short enough that the main part of the signal spectrum falls on frequencies less than twice the lower characteristic boundary frequency ν_L . This minimizes the influence of external feedback on the shape of the spectrum in its main part from which the motion parameters are determined.

Conflict of interest

The authors declare that they have no conflict of interest.

References

- [1] S.Kh. Pine, V.V. Kalugin, E.S. Kochurina. *Izvestiya vuz. Elektronika*, **28** (4), 452 (2023) (in Russian). DOI: 10.24151/1561-5405-2023-28-4-452-460
- [2] F. Levinzon. *Piezoelectric Accelerometers with Integral Electronics* (Springer International Publishing, NY., 2015)
- [3] V.I. Busurin, V.V. Korobkov, K.A. Korobkov, N.A. Koshevarova. *Izmeritelnaya tekhnika*, **11**, 34 (2020) (in Russian). DOI: 10.32446/0368-1025it.2020-11-34-41
- [4] E.B. Cooper, E.R. Post, S. Griffith, J. Levitan, S.R. Manalis, M.A. Schmidt. *Appl. Phys. Lett.*, **76** (22), 3316 (2000). DOI: 10.1063/1.126637
- [5] H.J. von Martens, A. Täubner, W. Wabinski, A. Link, H.J. Schlaak. *Measurement*, **28** (1), 3 (2000). DOI: 10.1016/S0263-2241(00)00003-8
- [6] A. Umeda, M. Onoe, K. Sakata, T. Fukushima, K. Kanari, H. Iioka, T. Kobayashi. *Sensors and Actuators A: Physical*, **114** (1), 93 (2004). DOI: 10.1016/j.sna.2004.03.011
- [7] I.A. Bunin, E.N. Kalish, D.A. Nosov, M.G. Smirnov, Yu.F. Stus. *Avtometriya*, **46** (5), 90 (2010) (in Russian).
- [8] L.F. Vitushkin, O.A. Orlov, A. Jermak, D. D'Agostino. *Izmeritelnaya tekhnika*, **3**, 3 (2012) (in Russian).
- [9] A.P. Kuznetsov, S.A. Kolesnikov, A.A. Golubev, K.L. Gubsky, S.V. Dudin, A.V. Kanzyrev, V.I. Turtikov, A.V. Utkin, V.V. Yakushev. *Pribory i tekhnika eksperimenta*, **3**, 116 (2011) (in Russian).
- [10] D. Guo, H. Jiang, L. Shi, M. Wang. *IEEE Photon. J.*, **10** (1), 6800609 (2018). DOI: 10.1109/JPHOT.2018.2792447
- [11] Y.J. Du, T.T. Yang, D.D. Gong, Y.C. Wang, X.Y. Sun, F. Qin, G. Dai. *Sensors*, **18** (7), 2055 (2018). DOI: 10.3390/s18072055
- [12] E.A. Mokrov, A.A. Papko. *Nano- i mikrosistemnaya tekhnika*, **1**, 3 (2002) (in Russian).
- [13] D.A. Usanov, A.V. Skripal, E.O. Kashchavtsev, S.Yu. Dobdin. *ZhTF*, **83** (7), 156 (2013) (in Russian).
- [14] O.I. Chanilov, D.A. Usanov, A.V. Skripal, A.S. Kamyshansky. *Technical Physics Letters*, **31** (21), 9 (2005) (in Russian).
- [15] D.A. Usanov, A.V. Skripal. *Poluprovodnikovye lazernye avtodiny dlya izmereniya parametrov dvizheniya pri mikro- i nanosmescheniyakh* (Izd-vo Saratovskogo un-ta, Saratov, 2014)
- [16] A.V. Skripal, S.Y. Dobdin, A.V. Dzhafarov, K.A. Sadchikov, I.A. Chernetsova. *Izvestiya Saratovskogo universiteta. Novaya seriya. Seriya: Fizika*, **19** (4), 279 (2019) (in Russian). DOI: 10.18500/1817-3020-2019-19-4-279-287
- [17] R. Lang, K. Kobayashi. *IEEE J. Quantum Electron*, **16** (3), 347 (1980). DOI: 10.1109/JQE.1980.1070479
- [18] G. Giuliani, M. Norgia, S. Donati, T. Bosch. *J. Opt. A: Pure Appl. Opt.*, **4** (6), 283 (2002). DOI: 10.1088/1464-4258/4/6/371

Translated by A.Akhtyamov